

Inhibitory Action of *Ilex paraguariensis* Extracts on the Corrosion of Carbon Steel in HCl Solution

Taissa F. Souza, Mariana Magalhães, Vanessa V. Torres and Eliane D'Elia *

Departamento de Química Inorgânica, Instituto de Química, Universidade Federal do Rio de Janeiro, Avenida Athos da Silveira Ramos 149, Centro de Tecnologia, Bloco A, CEP 21941-909, Cidade Universitária, Rio de Janeiro – RJ, Brazil

*E-mail: eliane@iq.ufrj.br

Received: 10 September 2014 / Accepted: 30 October 2014 / Published: 17 November 2014

The effect of *Ilex paraguariensis* extracts on the corrosion of carbon steel in 1 mol L⁻¹ HCl was examined. The efficiency for inhibiting the corrosion of C-steel in 1 mol L⁻¹ HCl increased as the extract concentration and immersion time increased. Polarization curves show that this extract act as mixed-type inhibitor with predominantly cathodic characteristics. The apparent activation energy (E_a) for the dissolution of C-steel slightly decreased when the extract was used. This result could be attributed to the chemisorption of the inhibitor onto the steel surface. The inhibitory property of the extract is discussed in terms of the mechanism by which its components adsorb onto the C-steel surface. This adsorption process obeyed a Langmuir adsorption isotherm. The phenolic components are not the only factor responsible for the inhibitory action of natural products.

Keywords: Carbon Steel, EIS, Polarization, Weight loss, Acid inhibition

1. INTRODUCTION

The use of inhibitors is one of the most practical methods to protect steel from corrosion, particularly in acidic solutions where preventing unexpected metal dissolution and acid consumption is critical [1-3]. The majority of inhibitors used in industry are organic compounds primarily composed of nitrogen, oxygen and sulfur atoms. Inhibitors that contain double or triple bonds play an important role in facilitating the adsorption of these compounds onto metal surfaces.² A bond can be formed between the electron pair and/or the π -electron cloud of the donor atoms and the metal surface, thereby reducing corrosive attack in acidic media. Although many of these compounds have high inhibition efficiencies, several have undesirable side effects, even at very low concentrations, due to their toxicity to humans, deleterious environmental effects, and high costs [1].

In recent years, interest has increased in the development and use of low-cost and eco-friendly compounds as corrosion inhibitors for mild steel [1-43]. Plant extracts are generally inexpensive and can be obtained through simple extraction processes. In our previous works, the effect of aqueous extracts of spent coffee grounds, garlic peels and fruit peels (mango, orange, passion fruit and cashew), and grape pomace on the corrosion of carbon steel in 1 mol L⁻¹ HCl was studied [1, 3-5].

The fresh leaves and stems of *Ilex paraguariensis* (green Yerba mate) are used to prepare the commercial product named “yerba mate”, which is used in North-Eastern Argentina, Southern Brazil and Eastern Paraguay to prepare a tea-like beverage named “mate” (infusions and decoctions) that is consumed by 30% of the population at a rate of 1 L/day. *I. paraguariensis* is popularly used as an antirheumatic and to treat gastrointestinal disorders because of its eupeptic and choleric properties. According to Bastos *et al.*, aqueous extracts of green Yerba mate (*Ilex paraguariensis*) and green tea (*Camellia sinensis*) are good sources of phenolic antioxidants, as previously described in the literature [44]. There are an increasing number patents for green mate products and a growing interest in this product by countries whose population do not traditionally consume these beverages [44-45]. Currently, green mate is exported to the United States, Europe and Asia as a vegetal drug or as extracts used in different phytopharmaceutical, food and cosmeceutic preparations.

The objective of this study was to investigate the effects of aqueous green Yerba mate extract as a corrosion inhibitor for carbon steel in a 1 mol L⁻¹ solution of hydrochloric acid. Open-circuit potential measurements, potentiodynamic polarization curves, electrochemical impedance measurements, and weight loss measurements were utilized for this purpose.

2. EXPERIMENTAL

2.1 Inhibitor preparation

Aqueous Yerba mate extracts were obtained by infusion. 5 g of Yerba mate (purchased from Herbal Ceni Mate Orgânico Ind. e Co. Ltda-ME) was ground in 100 mL of distilled water with an initial temperature of 100 °C for 60 minutes. This extract was then filtered, lyophilized, and stored at -4 °C prior to analysis. The lyophilized extract was used as a corrosion inhibitor for carbon steel in 1 mol L⁻¹ hydrochloric acid. Lyophilization is a dehydration process typically used to preserve a perishable material. This process works by freezing the material (in our case, the aqueous extract) and then reducing the surrounding pressure to allow the frozen water in the material to sublime directly from the solid phase to the gas phase. This procedure guarantees extract preservation because the greatly reduced water content inhibits the action of microorganisms and enzymes that would normally spoil or degrade the extract.

2.2 Solution preparation

The electrolyte was a 1 mol L⁻¹ HCl solution prepared from 37% m/v HCl (Merck Co., Darmstadt, Germany) and using double-distilled water. The experiments were carried out under non-

stirred and naturally aerated conditions. The concentration range of Yerba mate extract varied from 100 to 1000 mg of extract (inhibitor) per litre of electrolyte.

2.3 Electrochemical procedure

Working electrodes were prepared from steel specimens with the following composition (mass%): 0.18 C, 0.04 P, 0.05 S, 0.30 Mn, trace Si, and balanced with Fe. The electrodes were prepared by embedding steel rods in an epoxy resin and exposing a surface area of 1 cm² to the electrolyte. Prior to each measurement, the sample surfaces were abraded with 400, 600 and 1000 grade emery paper, washed with double-distilled water, degreased with acetone and dried in air.

All of the electrochemical measurements were conducted using a conventional three-electrode cylindrical glass cell at a temperature of 25 ± 2 °C. A saturated calomel electrode (SCE) and a large-area platinum wire were used as the reference and auxiliary electrodes, respectively.

In all experiments, the carbon steel electrode was allowed to reach the stable open-circuit potential (attained after 1 h). Electrochemical impedance measurements were performed over a frequency range of 100 kHz to 4 mHz at the stable open-circuit potential with an AC wave of 10 mV. Subsequently, the polarization curves were measured from the cathodic to the anodic direction from -300 mV below the open-circuit potential to 300 mV above it using a scan rate of 1.0 mV s⁻¹.

The electrochemical experiments were performed using an Autolab PGSTAT 128 N potentiostat/galvanostat, controlled by GPES/FRA electrochemical software (version 4.9) from Eco-Chemie (The Netherlands). The inhibition efficiency (*n*%) was calculated from both the potentiodynamic polarization curves and the electrochemical impedance diagrams, as shown in Eqs. (1) and (2), respectively:

$$n\% = \frac{j_{\text{corr},0} - j_{\text{corr}}}{j_{\text{corr},0}} \times 100 \quad (1)$$

where $j_{\text{corr},0}$ is the corrosion current density in the absence of inhibitor (blank) and j_{corr} is the corrosion current density in the presence of inhibitor, as obtained from Tafel plots.

$$n\% = \frac{R_{\text{ct}} - R_{\text{ct},0}}{R_{\text{ct}}} \times 100 \quad (2)$$

where $R_{\text{ct},0}$ is the charge-transfer resistance in the absence of inhibitor (blank) and R_{ct} is the charge-transfer resistance in the presence of inhibitor, as obtained from electrochemical impedance diagrams.

2.4 Weight loss measurements

C-steel specimens with the same composition as those used in the electrochemical measurements were mechanically cut, abraded with 100 grade emery paper, sandblasted, washed with double-distilled water, degreased with acetone, and dried in air. Triplicate specimens were immersed in the acid test solutions for 24 h at 25 °C in the absence and presence of 100, 200, 300, 400 and 1000 mg L⁻¹ aqueous Yerba mate extract obtained by infusion. The temperature was controlled using an aqueous thermostat. The specimens were removed, rinsed with water and acetone, dried in warm air

and stored in a desiccator. Weight loss was determined gravimetrically using an analytical balance with a precision of 0.1 mg. The inhibition efficiency ($n\%$) was obtained using Eq. (3)

$$n\% = \frac{W_0 - W}{W_0} \times 100 \quad (3)$$

where W_0 and W are the C-steel corrosion rates ($\text{g cm}^{-2} \text{h}^{-1}$) in the absence (blank) and presence of the extract, respectively.

The effects of time and temperature on the corrosion rate of steel coupons in 1 mol L^{-1} HCl were examined. These experiments were performed in the absence and presence of 100, 200, 300, 400 and 1000 mg L^{-1} aqueous Yerba mate extract for 4, 24 and 48 h at $25 \text{ }^\circ\text{C}$ and with an immersion period of 2 h at 25, 35, 45 and $55 \text{ }^\circ\text{C}$ for 200 mg L^{-1} of extract.

In the present study, each experiment was repeated three times under the same conditions, and the relative differences between replicate experiments were found to be less than 3%, indicating good reproducibility. The average of the three replicate values was used for further processing of the data.

2.5 Phenolic components of the extracts

The phenolic antioxidants of the Yerba mate extract were analyzed through the colorimetric determination of total phenolics via reaction with the Folin–Ciocalteu reagent. The analysis of the total phenolics in the aqueous extracts was conducted as described elsewhere [4, 46]. Freeze–dried samples were reacted with the Folin–Ciocalteu reagent, the level of absorbance was read at 760 nm using a DU Beckman Spectrophotometer (Beckman; CA, USA), and the contents of the total phenolics were expressed as mg of gallic acid equivalents per gram of freeze–dried extract (mg GAE/g).

2.6 Surface analysis

The specimens used for the surface morphology examination were immersed in 1 mol L^{-1} HCl in the absence (blank) and presence of 400 mg L^{-1} aqueous Yerba mate extract at $25 \text{ }^\circ\text{C}$ for 2 h. The analysis was performed using a Leo 940A (ZEISS) scanning electron microscope with an accelerating voltage of 20 kV.

3. RESULTS AND DISCUSSION

3.1. Electrochemical experiments

3.1.1. Potentiodynamic polarization curves

Figure 1 presents the potentiodynamic polarization curves of C-steel in 1 mol L^{-1} HCl in the absence and presence of 100, 200, 400 and 1000 mg L^{-1} aqueous Yerba mate extract at room temperature. The electrochemical parameters, i.e., the open-circuit potential (OCP), the corrosion

potential (E_{corr}), the corrosion current density (j_{corr}), and the anodic (β_a) and cathodic (β_c) Tafel constants, were obtained from the Tafel plots and are shown in Table 1.

The potentiodynamic polarization curves show that the presence of the extract caused a decrease in both the anodic and cathodic current densities, with a more pronounced decrease in the cathodic branch. These results could be explained by the adsorption of organic compounds present in the extracts at the active sites of the electrode surface, which also led to the retardation of metal dissolution and hydrogen evolution and consequently slowed the corrosion process.

As shown in Table 1, the corrosion current density (j_{corr}) decreased in the presence of the inhibitor. In the presence of the Yerba mate extract, both the OCP and the E_{corr} shifted to more cathodic potentials compared to the blank, demonstrating that this extract acts as a mixed-type inhibitor with predominantly cathodic characteristics. The cathodic (β_c) and anodic Tafel slopes (β_a) did not significantly change with the addition of the extract (Table 1). The inhibitor did not affect the mechanism of the anodic and cathodic reactions. Both the hydrogen evolution reaction and the metal dissolution reaction were exclusively diminished by the surface blocking effect. The inhibition efficiencies calculated from the j_{corr} values obtained in the absence and presence of Yerba mate extract varied from 71 to 79% over a concentration range of 100–1000 mg L⁻¹.

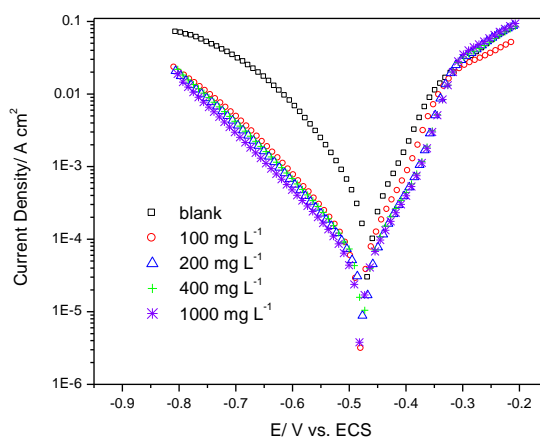


Figure 1. Polarization curves of C-steel in 1 mol L⁻¹ HCl in the absence and presence of varying concentrations of aqueous Yerba mate peel extract: 100, 200, 400 and 1000 mg L⁻¹.

Table 1. Kinetic parameters obtained from the Tafel plots for C-steel in 1 mol L⁻¹ HCl in the absence and presence of aqueous Yerba mate extract at the following concentrations: 100, 200, 400 and 1000 mg L⁻¹.

[Inhibitor] (mg L ⁻¹)	OCP (mV/SCE)	E_{corr} (mV/SCE)	j_{corr} (A cm ⁻²)	β_a mV dec ⁻¹	$-\beta_c$ mV dec ⁻¹	$n(\%)$
0	-456	-449	2.10×10^{-4}	62	102	-
100	-479	-474	6.08×10^{-5}	67	114	71
200	-473	-470	4.91×10^{-5}	73	120	77
400	-477	-472	5.60×10^{-5}	76	120	73
1000	-480	-474	4.35×10^{-5}	77	123	79

3.1.2. Electrochemical impedance spectroscopy (EIS)

The electrochemical impedance diagrams for C-steel in a 1 mol L⁻¹ HCl solution in the absence and presence of various concentrations of aqueous Yerba mate extract are shown in Figure 2. Table 1 summarizes the impedance data obtained from the EIS experiments conducted in both the absence and presence of increasing concentrations of extract. For the extract-free solution (Fig. 2A), only one depressed capacitive loop is observed, which is attributed to the time constant of the charge transfer and the double-layer capacitance. Deviations from a perfect circular shape indicate a frequency dispersion of the interfacial impedance. In the literature, this anomalous phenomenon is attributed to the nonhomogeneity of the electrode surface arising from surface roughness or interfacial phenomena [3]. This behavior is unaffected by the presence of inhibitor (Fig. 2B), indicating that the activation-controlled nature of the reaction is a single charge-transfer process. The solution resistance (R_s) is identical in the absence and presence of the Yerba mate extract, and it is equal to 1.4 Ω cm². The charge-transfer resistance (R_{ct}) values were calculated from the difference in impedances at lower and higher frequencies. The double-layer capacitance (C_{dl}) was calculated from the following equation:

$$C_{dl} = 1/(2\pi f_{max} R_{ct}) \quad (4)$$

where f_{max} is the frequency at which the imaginary component of the impedance is maximal.

A C_{dl} value of 45.5 μF cm⁻² was found for the C-steel electrode in 1 mol L⁻¹ HCl. From Table 1, it is clear that the R_{ct} values increased and that the C_{dl} values decreased as the concentration of inhibitor increased. This result indicates a decrease in the active surface area caused by the adsorption of the inhibitors on the carbon steel surface, and it suggests that the corrosion process became hindered; this hypothesis is supported by the anodic and cathodic polarization curves and by the corrosion potential results. The best result for the inhibition efficiency was obtained at a concentration of 1000 mg L⁻¹, with an efficiency equal to 91%.

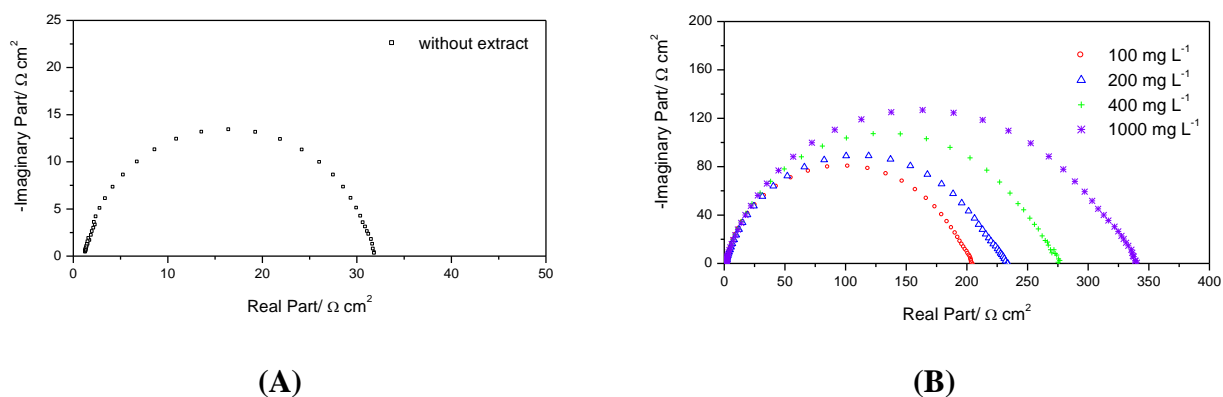


Figure 2. Impedance diagrams obtained at the corrosion potential for C-steel in 1 mol L⁻¹ HCl in the absence (A) and presence of aqueous Yerba mate extract with concentrations of 100, 200, 400 and 1000 mg L⁻¹ (B).

Inhibition efficiency is directly proportional to the fraction of the surface covered by the adsorbed molecules (θ), and it was calculated using the data obtained from the electrochemical impedance diagrams and the equation $\theta = n/100$ (see Eq. (2)).

The change in θ as a function of the extract concentration specifies the adsorption isotherm that describes the system (Figure 3). The fit of the obtained data to the Langmuir isotherm is illustrated by plotting according to equation (5). In this equation, C is the inhibitor concentration, θ is the occupied fraction of the surface, and K is the adsorption constant.

$$\frac{c}{\theta} = C + \frac{1}{K} \quad (5)$$

Table 2. Electrochemical parameters obtained from the EIS plots for C-steel in 1 mol L⁻¹ HCl in the absence and presence of aqueous Yerba mate extract at the following concentrations: 100, 200, 400 and 1000 mg L⁻¹.

Medium	[inhibitor] mg L ⁻¹	R _{ct} (Ω cm ²)	f _{max} (Hz)	C _{dl} (μF cm ⁻²)	n(%)
Without extract	-	30.6	114	45.5	-
With extract	100	203	114	6.88	85
	200	231	182	3.79	87
	400	276	230	2.51	89
	1000	338	291	1.62	91

Figure 3 shows linear plots with high correlation coefficients of 0.9999 and a slope of 1.08. This behavior suggests that the compounds present in the Yerba mate extract adsorbed onto the C-steel surface consistent with a Langmuir adsorption isotherm, indicating the absence of interaction forces between the adsorbed molecules.

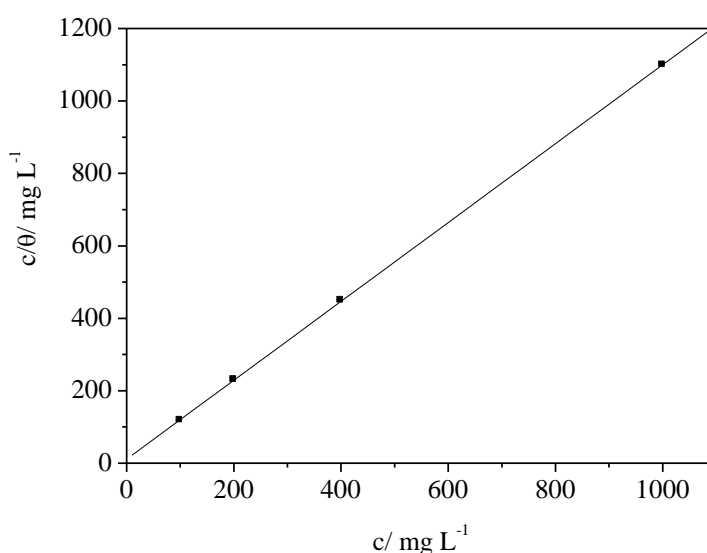


Figure 3. Langmuir adsorption isotherm for aqueous Yerba mate extract on a C-steel surface in a 1 mol L⁻¹ HCl solution.

Note that a discussion of the adsorption isotherm behavior using natural product extracts as inhibitors in terms of thermodynamic parameters (such as the standard free energy of adsorption value (ΔG_{ads})) is not possible because the molecular masses of the extract components are not known.

3.2. Weight loss measurements

The results from the weight loss measurements for the corrosion of C-steel in 1 mol L⁻¹ HCl in the absence and presence of different aqueous Yerba mate extract concentrations (100-1000 mg L⁻¹) for 4 and 24 h at 25 °C are provided in Table 3. The C-steel corrosion rate (W_{corr}) was greatly reduced upon the addition of the Yerba mate extract for all immersion times. The C-steel corrosion rate (W_{corr}) was dependent on the extract concentration and on the immersion time. As shown, $n\%$ increased as the Yerba mate extract concentration increased, varying from 51 to 80% in the concentration range of 100 to 1000 mg L⁻¹ for 4 h and from 65 to 93% for 24 h.

Moreover, these critical assays demonstrate the stability of the extract with time. Notably, there was an increase in the inhibition efficiency with time, from 80% after 4 h of immersion to 93% after 24 h of immersion in the presence of 1000 mg L⁻¹ of extract, which indicates that the inhibition efficiency remains high after long periods of immersion.

Table 1. C-steel weight loss in 1 mol L⁻¹ HCl in the absence and presence of aqueous Yerba mate extract at the following concentrations: 100, 200, 400 and 1000 mg L⁻¹ for 4 and 24 h at 25 °C.

Concentration (mg L ⁻¹)	W_{corr} (g cm ⁻² h ⁻¹)		$n\%$	
	4 h	24 h	4 h	24 h
Without Inhibitor	0.00259	0.00174	--	--
100	0.00126	0.00061	51	65
200	0.00087	0.00025	66	86
300	0.00076	0.00020	71	89
400	0.00066	0.00019	75	89
1000	0.00053	0.00012	80	93

The effects of temperature on the corrosion of C-steel in 1 mol L⁻¹ HCl, from 25 to 55 °C, after 2 h of immersion are presented in Table 4. The experiments were performed in the absence and presence of 200 mg L⁻¹ aqueous Yerba mate extract.

Table 2. C-steel weight loss in 1 mol L⁻¹ HCl in the absence and presence of 200 mg L⁻¹ of Yerba mate extract at the following immersion temperatures: 25, 35, 45, and 55 °C, with an immersion period of 2 h.

Temperature (°C)	W_{corr} (g cm ⁻² h ⁻¹) Without Inhibitor	W_{corr} (g cm ⁻² h ⁻¹) 200 mg L ⁻¹	n (%)
25	0.00322	0.001520	53
35	0.00489	0.002424	50
45	0.00869	0.004139	52
55	0.01299	0.005861	55

The corrosion rates of the steel in both free and inhibited acid media increased as the temperature increased, indicating that the presence of Yerba mate extract affected the C-steel corrosion process. Additionally, the inhibition efficiency of the Yerba mate extract remained quite constant with temperature.

The apparent activation energy for the corrosion of C-steel in free and in inhibited acid solution was determined from an Arrhenius-type plot according to Eq. (6):

$$\log W_{\text{corr}} = \frac{-E_a}{2.303RT} + \log A \quad (6)$$

where W_{corr} is the corrosion rate, E_a is the apparent activation energy, A is the frequency factor, T is the absolute temperature, and R is the ideal gas constant.

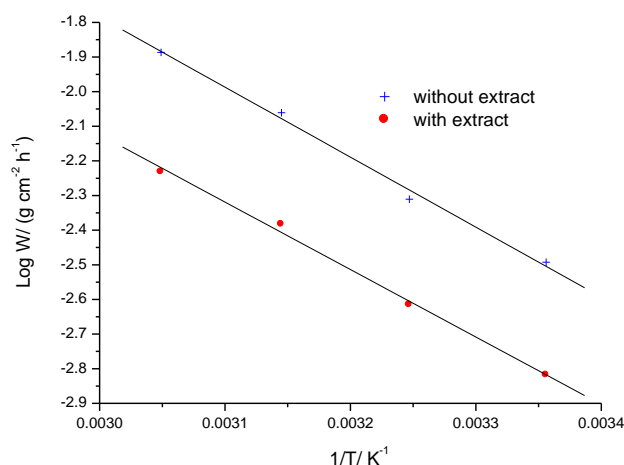


Figure 4. Arrhenius plots for the corrosion rate of C-steel in 1 mol L⁻¹ HCl solution in the absence and presence of Yerba mate extract.

Arrhenius plots of ($\log W_{\text{corr}}$) against ($1/T$) for C-steel in 1 mol L⁻¹ HCl, both in the absence and presence of the aqueous Yerba mate extract, are shown in Figure 4. The apparent activation energy obtained for the corrosion process in the free acid solution was found to be -38.7 kJ mol⁻¹, and it was found to be -37.3 kJ mol⁻¹ in the presence of the inhibitor. The energy barrier for the corrosion reaction slightly decreased in the presence of the inhibitor, whereas the inhibition efficiency remained almost

constant with various temperatures (Table 4). Such observations have been reported in other works and were explained by specific interactions between the steel surface and the inhibitor [43]. The lower value of E_a in the corrosion process in the presence of inhibitor compared to that in a free acid solution can be attributed to the chemisorption of the inhibitor onto the steel surface, involving charge sharing or charge transfer from the inhibitor molecules present in the Yerba mate peel extract to the C-steel surface.

3.3. Phenolic components in the Yerba mate extract

Phenolic compounds are substances normally found in Yerba mate samples and are generally considered to be the main antioxidant substances present in the extracts of natural products [44]. The total amount of phenolics found in the aqueous green mate was 293 mg/g. This value is higher than that in the extract of spent coffee grounds obtained using the infusion process (77.2 mg/g) [4]. This result is surprising because the inhibition efficiency obtained with 400 mg L⁻¹ spent coffee ground extract was higher (95%) than that obtained in the presence of 400 mg L⁻¹ green mate extract (89%) [4]. Therefore, this parameter cannot be the only factor responsible for the inhibitory action on the corrosion of carbon steel in the HCl solution.

3.4. Surface analysis

Figure 5 shows SEM micrographs of C-steel samples that were immersed in 1 mol L⁻¹ HCl for 2 h in the absence (Fig. 5A) and presence of 400 mg L⁻¹ aqueous Yerba mate extract (Fig. 5B) at 25 °C. The morphology in Fig. 5A shows a rough surface, characteristic of the uniform corrosion of C-steel in acid, as previously reported [1, 4]. In the presence of the Yerba mate extract (Fig. 5B), a smooth surface can be observed, indicating that the surface was covered by the inhibitor. These results corroborate the results from the electrochemical impedance spectroscopy and weight loss experiments.

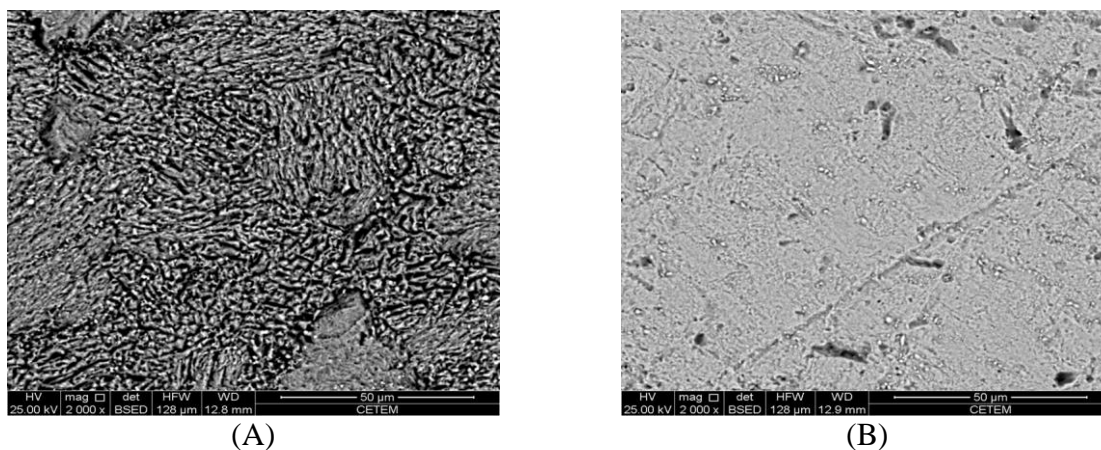


Figure 5. SEM micrographs (2000x) of C-steel immersed in 1 mol L⁻¹ HCl in the absence (A) and presence of 400 mg L⁻¹ aqueous Yerba mate extract (B).

4. CONCLUSIONS

Green mate extract acts as a corrosion inhibitor for C-steel in 1 mol L⁻¹ HCl solution. All of the electrochemical results, including the slight displacement in the corrosion potential, the inhibitory action in both the anodic and cathodic polarization curves, and the results of the electrochemical impedance measurements, indicated that the examined extract acted as an adsorption inhibitor on the C-steel surface. The efficiency of the extract in inhibiting the corrosion of C-steel in 1 mol L⁻¹ HCl increased with increasing extract concentration and immersion time and remained quite constant with changing temperature. The adsorption of the compounds in the Yerba mate extract followed the Langmuir adsorption isotherm. The apparent activation energy (E_a) for the dissolution of C-steel slightly decreased in the presence of the green mate extract. The SEM analysis revealed the formation of a smooth surface on C-steel in the presence of the Yerba mate extract compounds, which was most likely due to the formation of a strong chemisorptive bond between the Yerba mate extract compounds and the C-steel surface. Finally, the phenolic components are not the only factor responsible for the inhibitory action of natural products.

ACKNOWLEDGEMENTS

The authors thank Petrobras, CNPq and FAPERJ for financial support.

References

1. S.S.A.A. Pereira, M.M. Pegas, T. L. Fernandez, M. Magalhães, T.G. Schontag, D.C. Lago, L.F. de Senna, E. D'Elia, *Corros. Sci.*, 65 (2012) 360.
2. A. K. Satapathy, G. Gunasekaran, S. C. Sahoo, A. Kumar, P.V. Rodrigues, *Corros. Sci.*, 51 (2009) 2848.
3. J.C. da Rocha, J.A.C.P. Gomes, E. D'Elia, *Corros. Sci.*, 52 (2010) 2341.
4. V.V. Torres, R.S. Amado, C.F. de Sá, T.L. Fernandez, C.A.S. Riehl, A.G. Torres, E. D'Elia, *Corros. Sci.*, 53 (2011) 2385.
5. J.C. da Rocha, J.A.C.P. Gomes, E. D'Elia, A.P.G. Cruz, L.M.C. Cabral, A.G. Torres, M.V.C. Monteiro, *Int. J. Electrochem. Sci.*, 7 (2012) 11941.
6. K.S. Parikh, K.J. Joshi, *Trans. SAEST*, 39 (2004) 29.
7. P.B. Raja, M.G. Sethuraman, *Mater. Lett.*, 62 (2008) 2977.
8. P.B. Raja, M.G. Sethuraman, *Mater. Lett.*, 62 (2008) 113.
9. A. Spinelli, F.S. de Souza, *Corros. Sci.*, 51 (2009) 642.
10. A. Osvatori, S.M. Hoseinie, M. Peikar, S.R. Shadizadeh, S.J. Hashemi, *Corros. Sci.*, 51 (2009) 1935-1949.
11. A.Y. El-Etre, *J. Colloid Interface Sci.*, 314 (2007) 578.
12. P.C. Okafor, M.E. Ikpi, E.E. Ebenso, U.J. Ekpe, S.A. Umoren, *Corros. Sci.*, 50 (2008) 2310.
13. A.Y., El-Etre, M. Abdallah, Z.E. El-Tantawy, *Corros. Sci.*, 47 (2005) 385.
14. A.Y. El-Etre, *Appl. Surf. Sci.*, 252 (2006) 8521.
15. A.Y. El-Etre, *Mater. Chem. Phys.*, 108 (2008) 278.
16. I.H. Farooqi, A. Hussain, M.A. Quraishi, P.A. Saini, *Anti-Corros. Methods Mater.*, 46 (1999) 328.
17. A.M. Fekry, R.R. Mohamed, *Electrochim. Acta*, 55 (2010) 1933.
18. A.M. Abdel-Gaber, B.A. Abd-El-Nabey, I.M. Sidahmed, A.M. El-Zayady, M. Saadawy, *Corros. Sci.*, 48 (2006) 2765.

19. A.M. Abdel-Gaber, B.A. Abd-El-Nabey, M. Saadawy, *Corros. Sci.*, 51 (2009) 1038.
20. M.A. Quraishi, A. Singh, V.K. Singh, D.K. Yadav, A.K. Singh, *Mater. Chem. Phys.*, 122 (2010) 114.
21. A. Bouyanzer, B. Hammouti, L. Majidi, *Mater. Lett.*, 60 (2006) 2840.
22. L.R. Chauhan, G. Gunasekaran, *Corros. Sci.*, 49 (2007) 1143.
23. G. Gunasekaran, L.R. Chauhan, *Electrochim. Acta*, 49 (2004) 4387.
24. M.H. Hussin, M.J. Kassim, *Mater. Chem. Phys.*, 125 (2011) 461.
25. P. Kalaiselvi, S. Chellammal, S. Palanichamy, G. Subramanian, *Mater. Chem. Phys.*, 120 (2010) 643.
26. A. Lecante, F. Robert, P.A.;Blandinières, C. Roos, *Curr. Appl. Phys.*, 11 (2011) 714.
27. E.A. Noor, *Mater. Chem. Phys.*, 131 (2011) 160.
28. E. E.; Oguzie, *Mater. Chem. Phys.*, 99 (2006) 441.
29. E. E. Oguzie, *Corros. Sci.*, 50 (2008) 2993.
30. E.E. Oguzie, C.K. Enenebeaku, C.O. Akalezi, S.C. Okoro, A.A. Ayuk, E.N. Ejike, *J. Colloid Interface Sci.*, 349 (2010) 283.
31. P.C. Okafor, M.E. Ikpi, I.E. Uwah, E.E. Ebenso, U.J. Ekpe, S.A. Umoren, *Corros. Sci.*, 50 (2008) 2310.
32. K.O. Orubite, N.C. Oforka, *Mater. Lett.*, 58 (2004) 1768.
33. A. Ostovari, S.M. Hoseinieh, M. Peikari, S.R. Shadizadeh, S.J. Hashemi, *Corros. Sci.*, 51 (2009) 1935.
34. K.W. Tan, M.J. Kassim, *Corros. Sci.*, 53 (2011) 569.
35. U.M. Eduok, S.A. Umoren, A.P. Udoh, *Arabian J. Chem.*, 5 (2012) 325.
36. P.C. Okafor, V.I. Osabor, E.E. Ebenso, *Pigm.Res.Technol.*, 36 (2007) 299.
37. P.C. Okafor, U.J. Ekpe, E.E. Ebenso, E.E. Oguzie, N. S. Umo, A.R. Etor, *Trans. SAEEST*, 41 (2006) 82.
38. C. Kamal, M.G. Sethuraman, *Arabian J. Chem.*, 5 (2012) 155.
39. A.S. Yaro, A.A. Khadom, R.K Wael, *Alexandria Eng. J.*, 52 (2013) 129.
40. I.E. Uwah, P.C. Okafor, V.E. Ebiekpe, *Arabian J. Chem.*, 6 (2013) 285.
41. M.S. Al-Otaibi, A.M. Al-Mayouf, M. Khan, A.A. Mousa, S.A. Al-Mazroa, H.Z. Alkathlan, *Arabian J. Chem.*, 7 (2014) 340.
42. R.P. Bothi, R.A. Abdul, O. Hasnah, A. Khalijah, *Acta Phys. Chim. Sin.*, 26 (2010) 2171.
43. A. Bouyanzer, B. Hammouti, *Pigment Resin Technol.*, 33 (2004) 287.
44. D.H.M. Bastos, L.A. Saldanha, R.R. Catharino, A.C.H.F. Sawaya, I.B.S. Cunha, P.O. Carvalho, M.N. Eberlin, *Molecules*, 12 (2007) 423.
45. D.H.M. Bastos, E.Y. Ishimoto, M.O.M. Marques, A.F. Ferri, E.A.F.S. Torres, *J. Food Comp. Anal.*, 19 (2006) 538.
46. A.L. Waterhouse, *Current Protocols in Food Analytical Chemistry*, John Wiley & Sons, New York (2002).